Theor Chem Acc (2007) 117:637–647
DOI 10.1007/s00214-006-0197-y

REGULAR ARTICLE

Statistical mechanical modelling of chemical reactions in complex systems: the kinetics of the Haem carbon monoxide binding–unbinding reaction in Myoglobin

Andrea Amadei · Marco D'Abramo · Isabella Daidone · Maira D'Alessandro · Alfredo Di Nola · Massimiliano Aschi

Received: 4 September 2006 / Accepted: 13 October 2006 / Published online: 10 January 2007

Abstract The free energy profile and the (classical) kinetics of chemical reactions in (soft) condensed phase may be well modelled theoretically by means of molecular dynamics simulations, the perturbed matrix method (PMM) and statistical mechanics, as we provided in previous articles. In this paper, we describe the theoretical framework, discussing thoroughly its crucial points, and apply the model to an important biochemical reaction: the Haem carbon monoxide binding–unbinding reaction in Myoglobin, specifically investigating the reaction step involving the carbon–iron chemical bond formation (disruption) which is of particular biochemical interest.

Keywords Molecular dynamics · Perturbed matrix method · Statistical mechanics · Chemical kinetics · Carbon monoxide · Myoglobin

A. Amadei (✉)
Dipartimento di Scienze e Tecnologie Chimiche,
Università di Roma "Tor Vergata", via della Ricerca Scientifica, 00133 Rome, Italy
e-mail: andrea.amadei@uniroma2.it

M. D'Abramo · M. D'Alessandro · A. Di Nola
Dipartimento di Chimica,
Università di Roma "La Sapienza", P. le Aldo Moro 5, 00185 Rome, Italy

I. Daidone
Interdisciplinary Center for Scientific Computing,
University of Heidelberg, Im Neuenheimer Feld 368, 69120 Heidelberg, Germany

M. Aschi (✉)
Dipartimento di Chimica, Ingegneria Chimica e Materiali,
Università di l'Aquila, via Vetoio (Coppito 2), 67010 l'Aquila, Italy
e-mail: aschi@caspur.it

1 Introduction

One of the ultimate goals of theoretical–computational chemistry is the reliable modelling of chemical reactions in complex molecular systems. Among them, chemical reactions in proteins, because of the wide range of potential applications, probably represent the most appealing ones. When a biochemical reaction in a protein is concerned, the most serious problem to be faced is no longer, nowadays, the mechanical description of the macromolecular system, which can be addressed at reasonable computational cost using a certain number of approximations and computational tools [1–3]. Rather, the real technical–conceptual bottleneck is represented by the tremendous complexity of the configurational space accessible, at atomic level, by the overall system (including the solvent). Moreover, there is a further aspect which is to take into account. Beyond showing an intrinsic physical consistency, any valuable theoretical–computational approach must provide a reasonable model of the chemical reaction investigated. Hence, a comparison with experimental data is a necessary, and sometimes sufficient condition for validating a computational–theoretical method. For chemical reactions occurring within proteins, the typical experimental data available are kinetic measurements, i.e. macroscopic thermal rate coefficients. This aspect reinforces the complexity of the problem as macroscopic kinetic data arise from the average over an ensemble of trajectories in configurational space and cannot be treated through a simple and restricted mechanical–dynamical view. In this context, we have recently proposed a theoretical–computational approach [4] which is essentially developed within the statistical–mechanical framework by the use of the perturbed matrix method (PMM) [5–14] and

molecular dynamics (MD) simulations. The main aim of this approach is a rigourous evaluation of the free energy landscape for a given chemical event [12] and its use, within a diffusive model, for determining the relative rate coefficients. Such a model has been recently applied for a relatively simple reaction in solution [15]. In this paper, we show the theoretical framework of the model, discussing its fundamental features, and use such a method to describe in detail an important biochemical reaction. In particular our aim is the determination of the free energy landscape and related rate coefficients, for the Haem carbon monoxide (CO) binding–unbinding in Myoglobin (Mb). Such a reaction has received, in the last decades, an impressive deal of attention under a variety of experimental techniques [16–22]. From such experiments the CO–Mb binding reaction has been characterized as CO diffusion within Mb leading to a Haem–CO geminate pair eventually interconverting to the Haem–CO covalent complex. This last reaction step became, in the last years, one of the most investigated biochemical processes by means of computational–theoretical methods. Recent quantum chemical calculations, restricted to the isolated Haem–CO system, have definitely shown [23–25], that CO binding occurs upon spin inversion (quintet-singlet). More recently, a variety of computational attempts have been presented in order to describe such a reaction including, at different level of approximation, the protein-solvent effects [26–29]. However, such data are typically based on either a simplified description of the environment (e.g. using a mean field model or a very limited environment configurational sampling) or on a drastic simplification of the quantum mechanical description of the reaction centre (e.g. using semiempirical Hamiltonian terms) resulting often in an unreliable description of the chemical reaction. The PMM/MD model seems then very suited for combining a rather accurate quantum description of the electronic rearrangement in the reaction centre with an extended atomic configurational sampling, hence opening to the possibility of a complete equilibrium and non-equilibrium statistical mechanical description of a chemical reaction.

2 Theory

Defining with $\boldsymbol{r}_n$ the nuclear coordinates of the quantum centre (QC) (i.e. the system treated quantum mechanically) and $\boldsymbol{x}$ the coordinates of the atoms providing the (classical) perturbing field we can write, within certain approximations [6,8], the QC electronic (perturbed) Hamiltonian matrix as

$$\tilde{H}(\boldsymbol{r}_n,\boldsymbol{x}) \cong \tilde{H}^0(\boldsymbol{r}_n) + q_T\mathcal{V}(\boldsymbol{r}_0,\boldsymbol{x})\tilde{I} + \tilde{Z}_1(\boldsymbol{E}(\boldsymbol{r}_0,\boldsymbol{x}),\boldsymbol{r}_n) + \Delta V(\boldsymbol{r}_n,\boldsymbol{x})\tilde{I} \quad (1)$$

where $\tilde{H}^0(\boldsymbol{r}_n)$ is the unperturbed Hamiltonian matrix which can be constructed carrying out standard electronic structure calculations on the isolated QC, $\mathcal{V}(\boldsymbol{r}_0,\boldsymbol{x})$ and $\boldsymbol{E}(\boldsymbol{r}_0,\boldsymbol{x})$ are the (perturbing) electric potential and electric field at a given QC $\boldsymbol{r}_0$ position (typically the mass or geometrical centre), $\tilde{Z}_1(\boldsymbol{E},\boldsymbol{r}_n)$ is a perturbation matrix explicitly given by $[\tilde{Z}_1]_{l,l'} = -\boldsymbol{E}\cdot\langle\Phi_l^0|\hat{\boldsymbol{\mu}}|\Phi_{l'}^0\rangle$, $\Delta V(\boldsymbol{r}_n,\boldsymbol{x})$ approximates the perturbation due to all the higher order terms as a simple short-range potential and q_T is the QC total charge. Moreover, Φ_l^0 are the unperturbed (electronic) Hamiltonian eigenfunctions and all the matrices used are expressed in this unperturbed basis set. At each MD frame, the electric potential and field exerted by the environment can be evaluated (typically using the environment atomic charge distribution) and the perturbed Hamiltonian matrix constructed and diagonalized. Hence, a trajectory of the QC perturbed Hamiltonian eigenvalues and eigenvectors is obtained. Such calculations carried out along the reaction coordinate provide, within certain approximations and for a highly diluted QC [4], the reaction free energy and whatever electronic property at a generic reaction coordinate position η (for the sake of simplicity, we consider a single reaction coordinate). According to the theoretical model described in the previous paper [4], the (Helmholtz) free energy change for the reaction coordinate transition $\eta_{ref} \rightarrow \eta$ (providing the reaction standard chemical potential $\Delta\mu^{\ominus}$ as in our calculation the QC density is invariant along the transition) and the average value of an electronic property χ at the position η, are

$$\Delta A(\eta) = \Delta\mu^{\ominus}(\eta) \cong -kT\ln\left\langle \mathrm{e}^{-\beta\Delta(\varepsilon'+q_T\mathcal{V})}\right\rangle_{\eta_{\mathrm{ref}}}^{0} \quad (2)$$

$$\langle\chi(\eta)\rangle \cong \frac{\left\langle \mathrm{e}^{-\beta\Delta(\varepsilon'+q_T\mathcal{V})}\chi(\eta)\right\rangle_{\eta_{\mathrm{ref}}}^{0}}{\left\langle \mathrm{e}^{-\beta\Delta(\varepsilon'+q_T\mathcal{V})}\right\rangle_{\eta_{\mathrm{ref}}}^{0}} \quad (3)$$

In the previous equations, ε' is the (ground state) eigenvalue of $\tilde{H}^0 + \tilde{Z}_1$ and $\Delta(\varepsilon' + q_T\mathcal{V})$ provides the energy change, for each MD frame, due to the transition along the reaction coordinate and in principle obtained energy minimizing the QC internal quantum degrees of freedom. Moreover, the subscript η_{ref} and the zero superscript mean that the averages are performed in the statistical ensemble with constrained reaction coordinate (at the reference position η_{ref}) and the system is in its vibrational ground state. The previous expressions are correct within the approximation that a small reactant to product displacement along the reaction

coordinate, does not affect the quantum vibrations and (classical) mass tensor determinant [4]. Moreover, for a rather rigid QC (i.e. where all the internal coordinates except the reaction coordinate may be treated as harmonic quantum degrees of freedom) we may consider that for each accessible configuration $\Delta(\varepsilon' + q_T\mathcal{V})$ is a function only of the reaction coordinate, i.e. it is independent of the other QC internal coordinates, and hence only the energy minimized structures along the reaction coordinate (obtained in vacuo) are necessary to provide the unperturbed properties for PMM calculations [4]. It is worth noting that in order to define a proper (single) reaction coordinate for describing the kinetics of the chemical process and not only its thermodynamics, we need to use a classical degree of freedom such that all its orthogonal coordinates are well equilibrated during its relaxation.[1] Hence, it is possible that according to the initial conditions of the kinetic relaxation (i.e. the coordinates/observables equilibrated at the beginning of the process) and the exact definition of the reactant and product states, different reaction coordinates should be used. This clearly also implies that a certain variation of the reaction free energy profile is possible, as a consequence of the different choice of the reaction coordinate and hence of the orthogonal planes used to obtain the corresponding free energy. In principle, each of these reaction coordinates, if properly defined, should provide the correct kinetic relaxation for the corresponding process. In the present study, we consider the iron to carbon distance as the proper reaction coordinate, hence assuming that the kinetic (classical) relaxation along such a degree of freedom occurs with all the other degrees of freedom equilibrated, i.e. the kinetics may be modeled as a diffusion along the free energy surface. Note that for a highly diluted solute, including the QC, the reaction free energy is independent of the solute roto-translational coordinates [4] and the solvent, provided an initial equilibrium condition, is expected to relax instantaneously in the ensemble of reactive trajectories at each reaction coordinate position [15].

When we consider systems where the reactant to product transition is relatively large and/or a quantum transition is involved (in the Haem–CO binding the spin transition), it may be worth evaluating the correction term providing the free energy change at η, due to the possible variation of the vibrational energies and (classical) mass tensor determinant from the corresponding values at η_{ref} [15]. Assuming, as usual, the partition function as factorized into a semi-classical part and a quantum vibrational one (given by the product of the molecular vibrational partition functions) and considering rigid solvent molecules (water) with hence a coordinate independent classical mass tensor, we may express such a free energy term $\Delta A_I(\eta)$, for systems where all of the QC internal coordinates orthogonal to the reaction coordinate may be treated as harmonic (quantum) degrees of freedom, as [4,30]

$$\Delta A_I(\eta) = -kT\ln\frac{Q_{v,\eta}\int \mathrm{e}^{-\beta[\Phi(\boldsymbol{x},\eta)+\Delta\mathcal{U}_{v,0}(\boldsymbol{x},\eta)]}[\det\tilde{M}(\eta)]^{1/2}\,\mathrm{d}\boldsymbol{x}}{Q_{v,\eta_{\text{ref}}}\int \mathrm{e}^{-\beta[\Phi(\boldsymbol{x},\eta)+\Delta\mathcal{U}_{v,0}(\boldsymbol{x},\eta_{\text{ref}})]}[\det\tilde{M}(\eta_{\text{ref}})]^{1/2}\,\mathrm{d}\boldsymbol{x}} \tag{4}$$

where $Q_{v,\eta}, Q_{v,\eta_{\text{ref}}}$ are the QC molecular quantum vibrational partition functions including all the orthogonal internal degrees of freedom, obtained at η and η_{ref}, respectively, and $\boldsymbol{x}$ are the environment (classical) coordinates. Moreover, $\tilde{M}(\eta)$ and $\tilde{M}(\eta_{\text{ref}})$ are the mass tensors associated to all the QC classical coordinates (i.e. rototranslational and reaction coordinates) as obtained at η and η_{ref}, Φ is the (classical) potential energy of the system and $\Delta\mathcal{U}_{v,0}$ is the system vibrational ground state energy shift from a reference value [4,30], typically negligible. Note that for a system where the quantum centre is a subpart of a molecule the previous vibrational partition functions and mass tensors should refer in principle to the whole molecule (solute). However, approximating the complete solute vibrational partition function and mass tensor determinant as the product of the QC and the rest of the solute parts, we may still use in the last equation the QC partition function and mass tensor determinant, thus simplifying considerably the calculations. Note also that the use of the QC complete classical mass tensor determinant implies that, as required in Eq. 4, we deal with the unconstrained ensemble [4].

Using the approximation $\Delta\mathcal{U}_{v,0}(\boldsymbol{x},\eta) \cong \Delta\mathcal{U}_{v,0}(\boldsymbol{x},\eta_{\text{ref}})$ we then obtain, for the perturbed QC,

$$\Delta A_I(\eta) \cong -kT\ln\frac{Q_{v,\eta}}{Q_{v,\eta_{\text{ref}}}} - \frac{kT}{2}\ln\frac{\det\tilde{M}(\eta)}{\det\tilde{M}(\eta_{\text{ref}})} \tag{5}$$

providing

$$\Delta A(\eta) = \Delta\mu^{\ominus}(\eta) \cong -kT\ln\left\langle \mathrm{e}^{-\beta\Delta(\varepsilon'+q_T\mathcal{V})}\right\rangle_{\eta_{\text{ref}}}^{0} - kT\ln\frac{Q_{v,\eta}}{Q_{v,\eta_{\text{ref}}}} - \frac{kT}{2}\ln\frac{\det\tilde{M}(\eta)}{\det\tilde{M}(\eta_{\text{ref}})} \tag{6}$$

where the QC vibrational partition function along the reaction coordinate can be in general obtained via

[1] In this paper, we do not consider reactive processes which may relax faster or at a similar rate than the environment as they typically may occur at very high temperature. However, for molecules involving slowly relaxing internal coordinates, it is possible that such slow modes must be somehow included in the definition of the reactive surface in order to describe properly the kinetics of the reaction and not only its thermodynamics.

the corresponding in vacuo frequencies, i.e. we consider the unperturbed frequencies as the reference frequencies used in the definition of the vibrational partition function [4,30]. Note that within the approximations used to obtain ΔA_I, no corrections are needed for the χ average.

A straightforward extension of the previous relations provides the reaction free energy for the Haem–CO binding–unbinding reaction in Mb, involving the quintet to singlet or singlet to quintet spin transition (the triplet is energetically unstable and hence can be neglected, see Methods). In fact for such a kind of reaction, we may write the free energy along the reaction coordinate relative to a given reference condition, e.g. the Haem–CO covalent complex where the quintet is virtually unaccessible, and appropriate to describe the reaction process, as are the corresponding singlet and quintet variations from the singlet reference value and we considered the (classical) mass tensor for a given η position as virtually unaffected by the magnetic transition. Note that we consider as usual that, at least within the reaction time scale, spin transitions which do not conserve the total spin z-component may be disregarded, i.e. they are virtually forbidden. Therefore in Eq. 10, we include a single quintet term corresponding to the quintet state with null spin z-component, hence neglecting the degeneracy due to the other quintet states and assuming, at least in the transition state (TS) region, that the considered spin transition has a much faster relaxation rate than the reaction kinetics.

Using a similar procedure, within the same level of approximation, we may also obtain the corresponding expression for the χ electronic property at η

$$\begin{aligned}\langle\chi(\eta)\rangle &= \frac{\mathrm{e}^{-\beta A_s(\eta)}\,\langle\chi_s(\eta)\rangle_s + \mathrm{e}^{-\beta A_q(\eta)}\,\langle\chi_q(\eta)\rangle_q}{\mathrm{e}^{-\beta A_s(\eta)} + \mathrm{e}^{-\beta A_q(\eta)}} \\ &\cong \frac{(Q_{v,s,\eta}/Q_{v,s,\eta_{\mathrm{ref}}})\left\langle \mathrm{e}^{-\beta\Delta_s(\varepsilon'+q_T\mathcal{V})}\chi_s(\eta)\right\rangle^0_{\eta_{\mathrm{ref}},s} + (Q_{v,q,\eta}/Q_{v,s,\eta_{\mathrm{ref}}})\left\langle \mathrm{e}^{-\beta\Delta_q(\varepsilon'+q_T\mathcal{V})}\chi_q(\eta)\right\rangle^0_{\eta_{\mathrm{ref}},s}}{(Q_{v,s,\eta}/Q_{v,s,\eta_{\mathrm{ref}}})\left\langle \mathrm{e}^{-\beta\Delta_s(\varepsilon'+q_T\mathcal{V})}\right\rangle^0_{\eta_{\mathrm{ref}},s} + (Q_{v,q,\eta}/Q_{v,s,\eta_{\mathrm{ref}}})\left\langle \mathrm{e}^{-\beta\Delta_q(\varepsilon'+q_T\mathcal{V})}\right\rangle^0_{\eta_{\mathrm{ref}},s}}\end{aligned}$$

$$\begin{aligned}\Delta A(\eta) &= -kT\ln\frac{\mathrm{e}^{-\beta A_s(\eta)} + \mathrm{e}^{-\beta A_q(\eta)}}{\mathrm{e}^{-\beta A_s(\eta_{\mathrm{ref}})} + \mathrm{e}^{-\beta A_q(\eta_{\mathrm{ref}})}} \\ &\cong -kT\ln\frac{\mathrm{e}^{-\beta A_s(\eta)} + \mathrm{e}^{-\beta A_q(\eta)}}{\mathrm{e}^{-\beta A_s(\eta_{\mathrm{ref}})}} \\ &= -kT\ln\left[\mathrm{e}^{-\beta\Delta_s A(\eta)} + \mathrm{e}^{-\beta\Delta_q A(\eta)}\right] \qquad (7)\end{aligned}$$

$$\Delta_s A(\eta) = A_s(\eta) - A_s(\eta_{\mathrm{ref}}) \qquad (8)$$

$$\Delta_q A(\eta) = A_q(\eta) - A_s(\eta_{\mathrm{ref}}) \qquad (9)$$

providing, with the use of Eq. 6,

$$\begin{aligned}\Delta A(\eta) \cong -kT\ln\Bigg[&\frac{Q_{v,s,\eta}}{Q_{v,s,\eta_{\mathrm{ref}}}}\left\langle \mathrm{e}^{-\beta\Delta_s(\varepsilon'+q_T\mathcal{V})}\right\rangle^0_{\eta_{\mathrm{ref}},s} \\ &+\frac{Q_{v,q,\eta}}{Q_{v,s,\eta_{\mathrm{ref}}}}\left\langle \mathrm{e}^{-\beta\Delta_q(\varepsilon'+q_T\mathcal{V})}\right\rangle^0_{\eta_{\mathrm{ref}},s}\Bigg] \\ &-\frac{kT}{2}\ln\frac{\det\tilde{M}(\eta)}{\det\tilde{M}(\eta_{\mathrm{ref}})} \qquad (10)\end{aligned}$$

where the subscripts s, q refer to the singlet and quintet magnetic state, respectively,

$$\begin{aligned}\Delta_s(\varepsilon'+q_T\mathcal{V}) &= \varepsilon'_s(\eta) - \varepsilon'_s(\eta_{\mathrm{ref}}) \\ &\quad + q_T\left[\mathcal{V}(\boldsymbol{r}_0(\eta)) - \mathcal{V}(\boldsymbol{r}_0(\eta_{\mathrm{ref}}))\right] \\ \Delta_q(\varepsilon'+q_T\mathcal{V}) &= \varepsilon'_q(\eta) - \varepsilon'_s(\eta_{\mathrm{ref}}) \\ &\quad + q_T\left[\mathcal{V}(\boldsymbol{r}_0(\eta)) - \mathcal{V}(\boldsymbol{r}_0(\eta_{\mathrm{ref}}))\right]\end{aligned}$$

It must be noted that it is often possible to define the chemical states along the reaction coordinate such that the corrections provided by the ΔA_I terms are negligible, by restricting the allowed fluctuation range of a set of QC vibrational modes (i.e. constructing the corresponding mode partition functions considering only the vibrational states with energies lower than a given upper limit). This may be of particular interest when, as for the present case, in the chemical transition considered a limited set of quantum vibrational modes may become semi-classical anharmonic degrees of freedom, hence not allowing a proper use of the previous equations without restricting such modes within a confined (harmonic) fluctuation range. In such cases it is possible to define for these modes a reaction coordinate dependent fluctuation range ensuring a virtually instantaneous relaxation of the modes during the reaction and, within a good approximation, negligible corrections. Equation 10 thus reduces to

$$\begin{aligned}\Delta A(\eta) \cong -kT\ln\Bigg[&\left\langle \mathrm{e}^{-\beta\Delta_s(\varepsilon'+q_T\mathcal{V})}\right\rangle^0_{\eta_{\mathrm{ref}},s} \\ &+\left\langle \mathrm{e}^{-\beta\Delta_q(\varepsilon'+q_T\mathcal{V})}\right\rangle^0_{\eta_{\mathrm{ref}},s}\Bigg] \qquad (11)\end{aligned}$$

which we used to evaluate the reaction free energy of the Haem–CO binding–unbinding in Mb. Note that for

this reaction no significant variation of the mass tensor is present and only a few QC vibrational modes involving the CO rototranslations needed to be confined. Such a mode confinement, only relevant in the geminate complex η range, simply defined the proper geminate complex to be used in the reaction modelling.

Finally, using the reaction free energy profile and the diffusion coefficient D of the reaction coordinate (if available), it is possible to obtain the reaction (classical) kinetics by solving a diffusion equation [31] (DE, see Appendix) in the reaction coordinate space

$$\left(\frac{\partial\rho}{\partial t}\right)_\eta = \frac{D}{kT}\left[\rho\frac{\mathrm{d}^2\Delta\mu^\ominus}{\mathrm{d}\eta^2} + \frac{\mathrm{d}\Delta\mu^\ominus}{\mathrm{d}\eta}\left(\frac{\partial\rho}{\partial\eta}\right)_t\right] + D\left(\frac{\partial^2\rho}{\partial\eta^2}\right)_t \tag{12}$$

where $\rho(t,\eta)$ is the probability density in η and we assumed $\partial D/\partial t, \partial D/\partial\eta \cong 0$.

The time–space behaviour of ρ can provide in principle all the kinetic/thermodynamic information on the chemical reaction. Therefore, in order to schematize the kinetic process, we may define three chemical states: the TS defined by a tiny interval $[\eta_{TS}-\delta, \eta_{TS}+\delta]$ (typically about 0.1Å) centred on the reaction free energy maximum η_{TS}, the reactant (R) defined by one of the η range neighbour to the TS (here the right one), and the product (P) defined by the other neighbour η range (here the left one). Hence, within such a scheme the complete reaction can be described by the time dependence of these three chemical state probabilities, as obtained by

$$P_{TS}(t) = \int_{\eta_{TS}-\delta}^{\eta_{TS}+\delta} \rho(t,\eta)\,\mathrm{d}\eta \tag{13}$$

$$P_R(t) = \int_{\eta_{TS}+\delta}^{\eta_\mathrm{U}} \rho(t,\eta)\,\mathrm{d}\eta \tag{14}$$

$$P_P(t) = \int_{\eta_\mathrm{L}}^{\eta_{TS}-\delta} \rho(t,\eta)\,\mathrm{d}\eta \tag{15}$$

where $\eta_\mathrm{L}, \eta_\mathrm{U}$ are the lower and upper limits of the reaction coordinate range used to define the complete reaction. Note that as the η range is finite $\Delta\mu^\ominus$ used in the diffusion equation must provide two infinite free energy barriers at the extremes of such a range. These infinite barriers do not correspond in general to physical free energy barriers, they are used simply to restrict the reaction kinetics to the chemical step of interest. Once we obtain $P_{TS}(t), P_R(t), P_P(t)$ by the DE solution [15], we may construct a kinetic model via the following procedure. Consider the general reaction scheme for the three chemical states R, P and TS

$$R \overset{k_1}{\rightarrow} TS \overset{k_{-2}}{\rightarrow} P \tag{16}$$

$$P \overset{k_2}{\rightarrow} TS \overset{k_{-1}}{\rightarrow} R \tag{17}$$

and the stationary condition

$$\dot{P}_{TS} = k_1 P_R - k_{-1}P_{TS} + k_2 P_P - k_{-2}P_{TS} \cong 0 \tag{18}$$

$$P_{TS} \cong \frac{k_1 P_R + k_2 P_P}{k_{-1} + k_{-2}} \tag{19}$$

valid for $t \geq t_0$ (t_0 is the time interval required to achieve the steady state), providing

$$\dot{P}_R \cong -K_R P_R + K_P P_P \tag{20}$$

$$\dot{P}_P \cong K_R P_R - K_P P_P \tag{21}$$

$$K_R = \frac{k_{-2}k_1}{k_{-1}+k_{-2}} \tag{22}$$

$$K_P = \frac{k_{-1}k_2}{k_{-1}+k_{-2}} \tag{23}$$

where K_R and K_P can be considered as the rate constants for the $R \rightarrow P$ and $P \rightarrow R$ transitions, respectively.

From the obvious relation $1 = P_R(t) + P_P(t) + P_{TS}(t)$, we have $P_P(t) = 1 - P_R(t) - P_{TS}(t)$ and hence $\forall t \geq t_0$

$$P_{TS}(t) \cong \frac{(k_1 - k_2)P_R + k_2}{k_{-1} + k_{-2} + k_2} \tag{24}$$

$$\dot{P}_R \cong -KP_R + K' \tag{25}$$

$$K = \frac{k_1k_{-2} + k_1k_2 + k_2k_{-1}}{k_{-1} + k_{-2} + k_2} \tag{26}$$

$$K' = \frac{k_2k_{-1}}{k_{-1} + k_{-2} + k_2} \tag{27}$$

The general solution of the previous ordinary linear differential equation is, in the time range $t \geq t_0$,

$$P_R(t) \cong P_R(\infty) + [P_R(t_0) - P_R(\infty)]\ \mathrm{e}^{-K(t-t_0)} \tag{28}$$
$$P_R(\infty) = \frac{K'}{K} = \frac{k_2k_{-1}}{k_1k_{-2} + k_1k_2 + k_2k_{-1}}$$

From the last expressions, we readily obtain (using again $P_P(t) = 1 - P_R(t) - P_{TS}(t)$ and the stationary condition)

$$P_P(t) \cong P_P(\infty) - \frac{k_{-1} + k_{-2} + k_1}{k_{-1} + k_{-2} + k_2}\,[P_R(t_0) - P_R(\infty)]\ \mathrm{e}^{-K(t-t_0)} \tag{29}$$

$$P_P(\infty) = \frac{k_{-1} + k_{-2} - (k_{-1} + k_{-2} + k_1)P_R(\infty)}{k_{-1} + k_{-2} + k_2}$$

$$= \frac{k_1 k_{-2}}{k_1 k_{-2} + k_1 k_2 + k_2 k_{-1}}$$

$$P_{TS}(t) \cong P_{TS}(\infty) + \frac{k_1 - k_2}{k_{-1} + k_{-2} + k_2} [P_R(t_0) - P_R(\infty)]\ \mathrm{e}^{-K(t-t_0)} \quad (30)$$

$$P_{TS}(\infty) = \frac{(k_1 - k_2)P_R(\infty) + k_2}{k_{-1} + k_{-2} + k_2} = \frac{k_1 k_2}{k_1 k_{-2} + k_1 k_2 + k_2 k_{-1}}$$

It is also instructive to consider two special cases of this general model. If we deal with a reaction where $k_2 \cong 0$ then we have $K \cong K_R = k_1 k_{-2}/(k_{-1} + k_{-2})$ and

$$\frac{P_{TS}}{P_R} \cong \frac{k_1}{k_{-1} + k_{-2}} \quad (31)$$

corresponding to a simple steady state for the $R \rightarrow P$ reaction alone. This case is typical in systems where the free energy of the product is much lower than the reactant one or the product is instantaneously removed in some way (e.g. in enzymatic reactions). When $k_2, k_{-2} \cong 0$ we obtain a further condition with $K \cong k_1 k_{-2}/k_{-1}$ and $P_{TS}/P_R \cong k_1/k_{-1}$ which clearly corresponds to a pre-equilibrium between the R and TS species, as required by the Eyring theory. However, this last case is rather unusual as k_{-2} is typically larger than or of the same order of k_{-1} when $k_1 \gg k_2$, and hence the Eyring theory should not be used as a general model to describe chemical reactions.

3 Quantum chemical calculations and molecular dynamics simulations

All the quantum chemical calculations on the isolated His–Haem–CO complex, i.e. our quantum centre (see Fig. 1), were carried out using the Gaussian 98 [32] and Gamess US [33] packages. The reaction coordinate, i.e. the iron-carbon (Fe–CO) distance, was used to define a 6 points grid starting from the unperturbed potential energy minimum (located on the singlet surface at 1.8Å). Such a grid was used to evaluate the unperturbed (i.e. in vacuo) minimum energy structures up to 3.8 Angstrom Fe–CO distance. This procedure was performed for the singlet, quintet and triplet magnetic states. The triplet however, resulting systematically much higher in energy, was neglected in our PMM calculations. This procedure was carried out in the framework of Density Functional Theory using Becke's three parameters [34] exchange

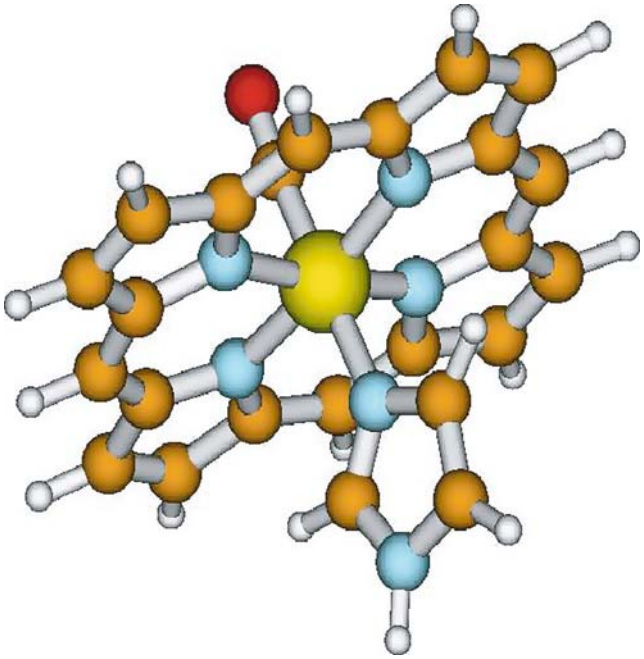

Fig. 1 Quantum centre used in our PMM calculation (reaction centre), defined by the Haem–CO complex and including the proxymal Histidine side chain. The figure refers to the reference QC condition, i.e. with the Haem–CO distance at 1.8Å

and the Lee et al. [35] correlation functionals (B3LYP) in conjunction with different atomic basis sets: for iron atom we used the Effective Core Potential from Los Alamos and a double-zeta basis set for the core and valence electrons, respectively; for the atoms bound to iron (four nitrogens and CO) the triple zeta 6-311++G(p,d) basis set was used and, finally, for the remaining atoms we used the 6-31G basis set. In order to apply PMM at each structure of the above reaction path, the electronic ground and the first nine excited energies as well as the corresponding (transition) dipoles, were then obtained carrying out Configuration Interaction with Single and Double excitations (CISD) using as reference state (reference Slater determinant) the one obtained by the previous B3LYP ground state evaluation. Such calculations provided the unperturbed Hamiltonian eigenstates defining the basis set used to construct the perturbed Hamiltonian matrix, which was then diagonalized for each simulation frame, at each Fe–CO distance leading to the reaction free energy and related properties. For this purpose N,V,T MD simulations were performed at 300 and 293 K, constraining Mb–CO in the centre of the simulation box, filled with 6,741 simple point charge [36] water molecules, at a liquid density (49.1 mol/l) determined by an initial 1.0 bar isobaric–isothermal equilibration run. All the simulations were performed using the Gromacs package [37–39]. Note that no experimental kinetic data for the reaction studied are available at 300 K and therefore, in order to somehow compare with

experimental rate constants, we decided to investigate this reaction at the closest temperature with available experimental data, i.e. at 293 K. The parameters describing the His–Haem–CO force field for the reference condition used in the MD simulations (i.e. the singlet Haem–CO covalent complex of the unperturbed QC) were determined as follows: the charges were recalculated adopting fitting procedures from previous B3LYP calculations [40]; for the other non-bonding and all the bonding interactions, we used the parameters contained in the Gromos force field [39] designed for similar atoms. Bond lengths were constrained by LINCS [41] and the rototranslational constraints [42] were used to keep the Mb–CO rototranslationally fixed at the centre of the simulation box. The temperature was kept constant using the isokinetic temperature coupling [43] in order to obtain results fully consistent with statistical mechanics [44] and the time step was of 2 fs. The long range electrostatics was calculated using the particle mesh ewald (PME) method [45], with 34 wave vectors in each dimension and a fourth order cubic interpolation. After the initial equilibration we used 10-ns runs to collect the data. In order to explicitly evaluate the (classical) kinetics of the Haem–CO binding (provided by the diffusion along the reaction free energy surface, using as initial condition a probability density confined in the energy minimum of the R state), we first evaluated the diffusion coefficient associated to the chosen reaction coordinate, i.e. the carbon–iron distance. For this purpose we performed (by Gromacs) two 110 ps MD trajectories at constant energy (i.e. with no temperature coupling) of the system, utilizing unconstrained bond lengths (with the corresponding Gromacs stretching parameters) and thus a reduced time step of 0.1 fs, starting from a MD frame of the 10-ns simulations either at 300 or 293 K (i.e. with the isokinetic temperature coupling), chosen so that its total energy was virtually identical to the value obtained by averaging over the corresponding 10-ns simulation. For the rest, these simulations were performed identically to the previous ones. Note that in both simulations the first 10 ps were considered as equilibration and hence removed from the analysis. Using a large number of (constant energy) trajectory subparts starting close to the carbon–iron equilibrium distance, we evaluated the reaction coordinate diffusion coefficient via the corresponding computed carbon-iron distance mean square displacement in time. Note that for a fast velocity autocorrelation function relaxation, as in the present case where the diffusive regime is achieved within a few femtoseconds, the use of a constant energy simulation to evaluate the diffusion coefficient is physically more consistent than using a constant temperature one. The obtained diffusion coefficient (about 4.2 10^{-3} nm^2/ps) was then utilized to solve (numerically) the diffusion equation (note that we assume a reaction coordinate independent diffusion coefficient which then may be obtained considering only the Haem–CO covalent complex ensemble). Finally, another constant temperature MD simulation (20 ns) was performed at 300 K for a system identical to the previous one except for the distal Histidine protonation site. In fact, in the former simulations we used the protonation site (nitrogen ϵ) considered as the proper one by the most recent data [28,46], while in the latter simulation we used the nitrogen δ protonation site previously considered as the correct one [47,48] and hence utilized in Mb MD simulations up to very recent years. This was done to evaluate the possible effects of the distal Histidine protonation site.

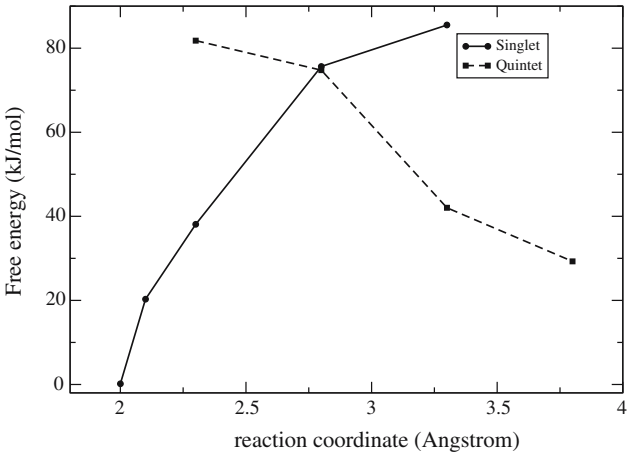

Fig. 2 Singlet and quintet reaction free energy surfaces, as obtained by PMM using the 293-K MD simulation

4 Results and discussion

In Fig. 2, we show the reaction free energy for the singlet and quintet surfaces (i.e. $\Delta_s A, \Delta_q A$) as obtained by PMM and MD simulations as described in the previous sections. Note that this figure refers to the data obtained by the 293-K MD simulation (distal Histidine protonated at nitrogen ϵ site). As for all the other simulations the reaction coordinate (i.e. Fe–CO distance) was fixed at 1.8Å (i.e. corresponding to the reference Haem–CO covalent complex). Similarly to the results for the isolated QC [25], the TS of the reaction in Mb is determined by the singlet–quintet free energy surface crossing. The triplet surface is thermodynamically too unstable to affect the reaction and, therefore, we omitted such a surface in our calculations. Interestingly, the perturbed QC free energy absolute minimum, at about 2.0Å, is slightly shifted from the unperturbed one (our

Table 1 Free energy barriers as obtained by different MD/PMM conditions as well as from in vacuo claculations

Ensemble	Binding barrier (kJ/mol)	Unbinding barrier (kJ/mol)
MD/PMM 300 K	43.8 ± 0.6	74.1 ± 0.9
MD/PMM 293 K	41.9 ± 0.6	74.2 ± 0.9
MD/PMM 300 K δ protonation site	41.4 ± 0.4	76.3 ± 0.7
DFT vacuum	47.6	87.6

The noise shown corresponds to a standard deviation

reference condition) indicating a corresponding slight variation of the Fe–CO equilibrium distance. It is also worth to note that the perturbed reference ground state (i.e. the perturbed singlet ground state at 1.8Å), as obtained by PMM, is virtually identical to the corresponding unperturbed ground state, showing that in the MD simulations the use of the unperturbed QC reference state atomic charges is fully consistent. In Table 1, we show the free energy barriers as obtained from the reaction free energy surfaces (Eq. 11) at the different temperatures also including the corresponding values for the isolated QC and the Mb with the distal Histidine protonated at nitrogen δ site. From the table, it is evident that the variation of the distal Histidine protonation site does not significantly affect the free energy barriers, and the protein provides a "catalytic" effect lowering the barriers of about 4–14 kJ/mol. Moreover, the free energy barriers at the two temperatures are, within the noise, almost identical suggesting low activation entropies, in line with previous results on a simple chemical reaction in solution [15]. Note that the free energy barriers we obtain are quite different from the values recently provided by another computational theoretical attempt to model the Haem–CO binding in Mb [49]. Such a discrepancy can be probably ascribed to the use of a purely semiempirical classical Hamiltonian for the reaction events which cannot properly describe the electronic rearrangements occurring during the chemical transition. In particular the binding free energy barrier reported in that article is far too small compared to our data, probably as a result of the use of the force field for the unbound CO [50] in the Haem–CO interaction.

In Fig. 3, we show the time dependence of the reactant (the geminate complex) and *TS* probabilities, obtained by the DE solution at 293 K. Note that in order to solve the diffusion equation we modelled $\Delta\mu^{\ominus}(\eta)$ by a simple polynomial function reproducing the PMM/MD free energy barriers, minima and *TS* positions, and for the system and time interval considered $P_R(t) - P_R(\infty) \cong P_R(t)$, $P_{TS}(t) - P_{TS}(\infty) \cong P_{TS}(t)$ (i.e. $P_R(\infty)$, $P_{TS}(\infty)$ are negligible). The figure demonstrates that the steady state model described in the theory section is very accurate to provide the kinetics of the reaction in terms of a simple reactant–*TS*–product scheme, as typically used to interpret experimental data. By using such time courses as well as the reactant to *TS* ($\Delta A_R^{\ddagger} = A_{TS} - A_R$) and product to *TS* ($\Delta A_P^{\ddagger} = A_{TS} - A_P$) free energy differences

$$\Delta A_R^{\ddagger} = -kT \ln \frac{P_{TS}(\infty)}{P_R(\infty)} = -kT \ln \frac{\int_{\eta_{TS}-\delta}^{\eta_{TS}+\delta} \mathrm{e}^{-\beta\Delta A(\eta)}\,\mathrm{d}\eta}{\int_{\eta_{TS}+\delta}^{\eta_U} \mathrm{e}^{-\beta\Delta A(\eta)}\,\mathrm{d}\eta}$$

$$\Delta A_P^{\ddagger} = -kT \ln \frac{P_{TS}(\infty)}{P_P(\infty)} = -kT \ln \frac{\int_{\eta_{TS}-\delta}^{\eta_{TS}+\delta} \mathrm{e}^{-\beta\Delta A(\eta)}\,\mathrm{d}\eta}{\int_{\eta_L}^{\eta_{TS}-\delta} \mathrm{e}^{-\beta\Delta A(\eta)}\,\mathrm{d}\eta}$$

it is possible to obtain all the kinetic rate constants involved in the reaction step studied (see theory section). In fact, from the overall rate constant $K = 3.4\ 10^{-7}\ \mathrm{ps}^{-1}$, evaluated by the slope of the logarithmic reactant decay, the *TS* probability at the beginning of the stationary condition (starting after 200–300 fs) and the relations $k_{-1} = k_1\ \mathrm{e}^{\beta\Delta A_R^{\ddagger}}, k_{-2} = k_2\ \mathrm{e}^{\beta\Delta A_P^{\ddagger}}$, we obtain the four rate constants for the reactant–*TS*–product interconversion which then provide for the reactant to product and inverse rate constants $K_R = 3.4\ 10^{-7}\ \mathrm{ps}^{-1}$, $K_P = 9.2\ 10^{-13}\ \mathrm{ps}^{-1}$ corresponding to about 3 μs and 1 s, respectively. Note that from our calculations $K_R \cong K$, as expected by the large free energy difference between the reactant and product states, and a rough estimate of the error of the K_R and K_P rate constants, essentially due to the noise in the free energy barriers, provides a maximal possible excursion (evaluated using ±4 standard deviations of the free energy barrier) corresponding to 0.7–12.0 μs and 0.3–3.0 s, respectively. Such results can be compared to the experimental data at 293 K [51,52], considering that the $R \rightarrow P$ and the $P \rightarrow R$ transitions are reaction steps involved in either the geminate binding kinetics (obtained after photolization of the Haem–CO covalent complex) or in the thermal Haem–CO dissociation. Interestingly, the experimental rate for the dissociation process is equal to $1.9\ 10^{-14}\ \mathrm{ps}^{-1}$ reasonably close, within the noise, to our K_P value (note that only 9–10 kJ/mol variation in the unbinding barrier would account for the ≃50 times variation of K_P with respect to the overall dissociation rate). This suggests that in the Haem–CO thermal dissociation the $P \rightarrow R$ transition (i.e. the Haem–CO chemical bond disruption) is probably the rate limiting step of the whole kinetic process, instead of the invoked slow conformational transitions [53,22]. In fact the supposed distal Histidine opening-closing side chain transition, often considered as the slow conformational change involved in the reac-

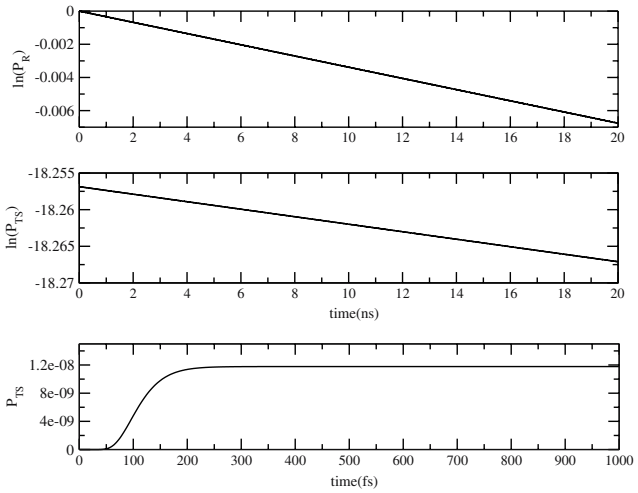

Fig. 3 Kinetics of the reactant (the geminate complex), upper panel, and transition, middle and lower panels, states as obtained by the DE solution for the system at 293 K

tion, results from our MD simulation data [54] as largely equilibrated within a few nanoseconds. Note that for the geminate binding, with an experimental rate constant of 5.6 10^{-6} ps^{-1} close to our K_R, no simple comparison is possible because of the complex non-sequential reaction scheme involved.

5 Conclusions

In this paper, we show that a proper statistical mechanical modelling of chemical reactions in complex systems can be achieved by combining the PMM and MD simulations. The extension of this method to treat chemical events involving different quantum reaction surfaces, introduced in the present paper, proved to be very efficient to describe the kinetics of a complex biochemical reaction: the Haem–CO geminate complex Haem–CO covalent complex interconversion in Mb.

Remarkably, the rate constants describing the binding–unbinding reactions are roughly comparable to the overall experimental rate constants suggesting that the geminate complex–covalent complex interconversion represents the rate limiting step. These results further show that a vast variety of chemical-kinetic events, ranging from simple reaction steps [4,12,15] to peptide folding–unfolding interconversion [55], can be reliably addressed in terms of diffusion over free energy surfaces.

Acknowledgments We gratefully acknowledge Dr. M. Pellegrino, Dr. N. Tantalo and 'Centro Ricerche Studi Enrico Fermi' (Roma, Italia) for computational support. We wish also to thank CASPUR (Roma, Italia) for allowing us to use Gaussian98. This work was carried out under the HPC-EUROPA project (RII3-CT-2003-506079), with the support of the European Community—Research Infrastructure Action of the FP6. Finally, we acknowledge the support of the grants from MIUR (PRIN 2005 on "Structure and dynamics of redox proteins").

Appendix

Here we show, in a simple and direct way, how to obtain the diffusion equation used in this paper.

Consider, in general, a set of reaction coordinates $\boldsymbol{\eta}$ providing the kinetic relaxation of the system, i.e. all the other degrees of freedom are assumed to be fully equilibrated along the $\boldsymbol{\eta}$ relaxation. The equations of motion for the $\boldsymbol{\eta}$ degrees of freedom when averaging over the ensemble defined by the molecules (typically the solute molecules) within a tiny $\boldsymbol{\eta}$ volume (equivalent to a numerical differential), can be approximated as

$$\left\langle \dot{\boldsymbol{\pi}}_{\eta}(\boldsymbol{\eta}) \right\rangle \cong \boldsymbol{F}(\boldsymbol{\eta}) - \tilde{\Gamma}(t,\boldsymbol{\eta}) \left\langle \boldsymbol{\pi}_{\eta}(\boldsymbol{\eta}) \right\rangle \tag{32}$$

$$\left\langle \boldsymbol{\pi}_{\eta}(\boldsymbol{\eta}) \right\rangle = \tilde{M}_{\eta,\eta}(\boldsymbol{\eta}) \left\langle \dot{\boldsymbol{\eta}}(\boldsymbol{\eta}) \right\rangle \tag{33}$$

where $\boldsymbol{\pi}_{\eta}$ are the $\boldsymbol{\eta}$ conjugated momenta, $\boldsymbol{F}$ is the systematic, i.e. equivalent to an external field, force in the $\boldsymbol{\eta}$ space and $\tilde{\Gamma}$, $\tilde{M}_{\eta,\eta}$ are the friction matrix and (classical) mass tensor block corresponding to the $\boldsymbol{\eta}$ coordinates. We assumed a virtually fixed mass tensor for a given $\boldsymbol{\eta}$ position and hence $\tilde{M}_{\eta,\eta}$ provides the only non-zero terms of $\boldsymbol{\pi}_{\eta}$ after averaging, as the other degrees of freedom are considered as fully equilibrated with hence zero mean velocities. Within the approximation given by the previous equations, the work due to the systematic force only should coincide with the maximum work along the transition, i.e. the work obtained for a reversible transition with then $\langle \dot{\boldsymbol{\eta}} \rangle = 0$. Hence, for a molecule passing from a tiny volume centred at $\boldsymbol{\eta}_a$ to another one centred at $\boldsymbol{\eta}_b$ we can write

$$\begin{aligned} \Delta A(\boldsymbol{n}) &= \left(\frac{\partial A}{\partial n_{\boldsymbol{\eta}_b}}\right) + \left(\frac{\partial A}{\partial n_{\boldsymbol{\eta}_a}}\right)\left(\frac{\partial n_{\boldsymbol{\eta}_a}}{\partial n_{\boldsymbol{\eta}_b}}\right) \\ &= \mu(n_{\boldsymbol{\eta}_b},\boldsymbol{\eta}_b) - \mu(n_{\boldsymbol{\eta}_a},\boldsymbol{\eta}_a) = -\int_{\boldsymbol{\eta}_a}^{\boldsymbol{\eta}_b} \boldsymbol{F}(\boldsymbol{\eta}) \cdot \mathrm{d}\boldsymbol{\eta} \end{aligned} \tag{34}$$

providing

$$\boldsymbol{F}(\boldsymbol{\eta}) = -\nabla_{\boldsymbol{\eta}} \mu(n_{\boldsymbol{\eta}},\boldsymbol{\eta}) \tag{35}$$

In the last equations, $A(\boldsymbol{n})$ is the Helmholtz free energy of the total NVT system fully defined by the vector $\boldsymbol{n} = n_{\boldsymbol{\eta}_1}, n_{\boldsymbol{\eta}_2}, \ldots$ providing the molecular number in each tiny volume and $\mu(n_{\boldsymbol{\eta}},\boldsymbol{\eta})$ is the chemical potential at a given $\boldsymbol{\eta}$ position, i.e. within the corresponding tiny volume. Note that the molecular number can be

used as a continuous variable, given the fact that for any thermodynamic property in a macroscopic system the variation due to a single molecule is virtually equivalent to a differential. From the definition of the chemical potential and probability density in the $\boldsymbol{\eta}$ space $\rho(t,\boldsymbol{\eta})$, we readily have

$$\mu(n_{\boldsymbol{\eta}},\boldsymbol{\eta}) = \Delta\mu^{\ominus}(\boldsymbol{\eta}) + kT\ln\frac{n_{\boldsymbol{\eta}}}{n_{\boldsymbol{\eta}_R}} + \mu(n_{\boldsymbol{\eta}_R},\boldsymbol{\eta}_R) \tag{36}$$

$$= \Delta\mu^{\ominus}(\boldsymbol{\eta}) + kT\ln\frac{\rho(t,\boldsymbol{\eta})}{\rho(t,\boldsymbol{\eta}_R)} + \mu(n_{\boldsymbol{\eta}_R},\boldsymbol{\eta}_R) \tag{37}$$

which used together with $\langle\dot{\boldsymbol{\pi}}_{\eta}\rangle \cong 0$ (the linear regime condition) provides

$$\langle\dot{\boldsymbol{\eta}}(\boldsymbol{\eta})\rangle \cong -\left[\tilde{\Gamma}(t,\boldsymbol{\eta})\tilde{M}_{\eta,\eta}(\boldsymbol{\eta})\right]^{-1}\nabla_{\boldsymbol{\eta}}\Delta\mu^{\ominus}(\boldsymbol{\eta}) - \left[\tilde{\Gamma}(t,\boldsymbol{\eta})\tilde{M}_{\eta,\eta}(\boldsymbol{\eta})\right]^{-1} kT\frac{\nabla_{\boldsymbol{\eta}}\rho(t,\boldsymbol{\eta})}{\rho(t,\boldsymbol{\eta})} \tag{38}$$

Hence from the definition of the flux density vector $\boldsymbol{J}(\boldsymbol{\eta}) = \rho(t,\boldsymbol{\eta})\,\langle\dot{\boldsymbol{\eta}}(\boldsymbol{\eta})\rangle$ and setting

$$\tilde{D}(t,\boldsymbol{\eta}) = kT\left[\tilde{\Gamma}(t,\boldsymbol{\eta})\tilde{M}_{\eta,\eta}(\boldsymbol{\eta})\right]^{-1} \tag{39}$$

we obtain, via the divergence theorem,

$$\left(\frac{\partial\rho}{\partial t}\right)_{\boldsymbol{\eta}} = -\nabla_{\boldsymbol{\eta}}\cdot\boldsymbol{J} \cong \nabla_{\boldsymbol{\eta}}\cdot\left[\tilde{D}(kT)^{-1}\rho\nabla_{\boldsymbol{\eta}}\Delta\mu^{\ominus} + \tilde{D}\nabla_{\boldsymbol{\eta}}\rho\right] \tag{40}$$

This last equation, when considering a one-dimensional $\boldsymbol{\eta}$ space with then $\tilde{D} = D$, provides the diffusion equation used in this paper within the assumption $\partial D/\partial t$, $\partial D/\partial\eta \cong 0$ (see theory section).

References

1. Shoneboom JC, Lin H, Reuter N, Thiel W, Cohen S, Ogliaro F, Shaik S (2002) J Am Chem Soc 124:8142–8151
2. Guallar V, Baik M, Lippard SJ, Friesner RA (2003) Proc Natl Acad Sci USA 100:6998–7002
3. Bathelt CM, Zurek J, Mulholland AJ, Harvey JN (2005) J Am Chem Soc 127:12900–12908
4. Amadei A, D'Alessandro M, Aschi M (2004) J Phys Chem B 108:16250
5. Aschi M, Spezia R, Di Nola A, Amadei A (2001) Chem Phys Lett 344:374
6. Spezia R, Aschi M, Di Nola A, Amadei A (2002) Chem Phys Lett 365:450
7. Spezia R, Aschi M, Di Nola A, Valentin MD, Carbonera D, Amadei A (2003) Biophys J 84:2805
8. Amadei A, Zazza C, D'Abramo M, Aschi M (2003) Chem Phys Lett 381:187
9. Aschi M, Zazza C, Spezia R, Bossa C, Di Nola A, Paci M, Amadei A (2004) J Comput Chem 25:974
10. D'Abramo M, Aschi M, Di Nola A, Amadei A (2005) Chem Phys Lett 402:559
11. Aschi M, D'Abramo M, Di Teodoro C, Di Nola A, Amadei A (2005) Chem Phys Chem 6:53
12. D'Alessandro M, Aschi M, Paci M, Di Nola A, Amadei A (2004) J Phys Chem B 108:16255
13. Amadei A, Marinelli F, D'Abramo M, D'Alessandro M, Anselmi M, Di Nola A, Aschi M (2005) J Chem Phys 122:124506
14. Di Teodoro C, Aschi M, Amadei A, Roccatano D, Malatesta F, Ottaviano L (2005) Chem Phys Chem 6:681–689
15. Aschi M, D'Abramo M, Ramondo F, Daidone I, D'Alessandro M, Di Nola A, Amadei A (2006) J Phys Org Chem 19:518
16. Austin RH, Beeson KW, Eisenstein L, Frauenfelder H, Gunsalus IC (1975) Biochemistry 14:5355
17. Steinbach PJ, Ansari A, Berendzen J, Braunstein D, Chu K, Cowen BR, Ehrenstein D, Frauenfelder H, Johnson JB, Lamb DC, Luck S, Mourant GU, Nienhaus GU, Ormos P, Philipp R, Xie AH, Young RD (1991) Biochemistry 30:3988
18. Srajer V, Ren Z, Teng TY, Schmidt M, Ursby T, Bourgeois D, Pradervand C, Schildkamp W, Wulff M, Moffat K (2001) Biochemistry 40:13802
19. Bourgeois D, Vallone B, Scotte F, Arcovito A, Miele AE, Sciara G, Wulff M, Anfinrud P, Brunori M (2003) Proc Natl Acad Sci USA 100:8704
20. Sottini S, Abbruzzetti S, Viappiani C, Ronda L, Mozzarelli A (2005) J Phys Chem B 109:19523–19528
21. Chen E, Goildberg RA, Kliger DS (1997) Annu Rev Biophys Biomol Struct 26:327
22. Angeloni L, Feis A (2003) Photochem Photobiol Sci 2:730–740
23. McMahon BH, Stojkovic BP, Hay PJ, Martin RL, Garcia AE (2000) J Chem Phys 113:6831
24. Franzen SJ (2002) Phys Chem B 106:4533
25. Harvey JN (2000) J Am Chem Soc 122:12401
26. Harvey JN (2004) Faraday Discuss 127:156
27. Sigfridsson E, Ryde UJ (2002) Inorg Biochem 91:101
28. De Angelis F, Jarzecki AA, Car R, Spiro TG (2005) J Phys Chem B 109:3065
29. Rovira C, Schultze B, Eichinger M, Evanseck JD, Parrinello M (2001) Biophys J 81:435
30. D'Abramo M, D'Alessandro M, Amadei A (2004) J Chem Phys 120:5226
31. McQuarrie DA (1976) Statistical mechanics. Harper Collins Publishers, New York
32. Gaussian 98 (Revision A.7), Gaussian, Inc., Pittsburgh PA (1998)
33. Schmidt MW, Baldridge KK, Boatz JA et al (1993) J Comput Chem 14:1347
34. Becke AD (1996) J Chem Phys 84:4524
35. Lee C, Yang W, Parr RG (1988) Phys Rev B 37:785
36. Feenstra KA, Hess B, Berendsen HJC (1999) J Comput Chem 20:786
37. van der Spoel D, van Drunen R Berendsen HJC, "GRoningen MAchine for Chemical Simulations", Department of Biophysical Chemistry, BIOSON Research Institute, Nijenborgh 4 NL-9717 AG Groningen (1994) e-mail: gromacs@chem.rug.nl
38. van der Spoel D, van Buuren AR, Apol E, Meulenhoff PJ, Tieleman DP, Sijbers ALT, van Drunen R, Berendsen HJC (1996) "Gromacs User Manual Version 1.3", 1996 Internet: http://rugmd0.chem.rug.nl/ gmx
39. van Gunsteren WF, Billeter SR, Eising AA, Hünenberger PH, Krüger K, Mark AE, Scott WRP, Tironi IG (1996) Biomolecular Simulation: The GROMOS96 Manual and User Guide; Hochschulverlag AG an der ETH Zürich:Zürich
40. Spackman MA (1996) J Comput Chem 17:1

41. Bekker B, Berendsen HJC, Fraije JGEM (1997) J Comp Chem 18:1463
42. Amadei A, Chillemi G, Ceruso MA, Grottesi A, Di Nola A (2000) J Chem Phys 112:9
43. Evans DJ, Morriss GP (1990) Statistical mechanics of non-equilibrium liquids. Academic, London
44. D'Alessandro M, Tenenbaum A, Amadei A (2002) J Phys Chem B 106:5050
45. Darden TA, York DM, Pedersen LG (1993) J Chem Phys 98:10089
46. Nienhaus K, Olson JS, Franzen S, Nienhaus GU (2005) J Am Chem Soc 127:4041
47. Kachalova GS, Popov AN, Bartunik HD (1999) Science 284:473
48. Schulze BG, Evanseck JD (1999) J Am Chem Soc 121:6444
49. Banushkina P, Meuwly M (2005) J Phys Chem B 109:16911–16917
50. Meuwly M, Becker OM, Stote R, Karplus M (2002) Biophys Chem 98:183
51. Springer BA, Sligar SG, Olson SJ, Phillips JN Jr (1994) Chem Rev 94:699–714
52. Olson SJ, Phillips JN Jr (1996) J Biol Chem 271:17593–17596
53. Kleinert T, Doster W, Leyser H, Petry W, Schwarz W, Settles M (1998) Biochemistry 37:717–733
54. Bossa C, Anselmi M, Roccatano D, Amadei A, Vallone B, Brunori M, Di Nola A (2004) Biophys J 86:3855–3862
55. Daidone I, D'Abramo M, Di Nola A, Amadei A (2005) J Am Chem Soc 127:14825